High performance nonvolatile memory devices based on Cu2−xSe nanowires

Chun-Yan Wu, Yi-Liang Wu, Wen-Jian Wang, Dun Mao, Yong-Qiang Yu, Li Wang, Jun Xu, Ji-Gang Hu, and Lin-Bao Luo

Citation: Applied Physics Letters **103**, 193501 (2013); doi: 10.1063/1.4828881
View online: http://dx.doi.org/10.1063/1.4828881
View Table of Contents: http://scitation.aip.org/content/aip/journal/apl/103/19?ver=pdfcov
Published by the AIP Publishing

High performance nonvolatile memory devices based on $Cu_{2-x}Se$ nanowires

Chun-Yan Wu (吴春艳),[a] Yi-Liang Wu (吴义良), Wen-Jian Wang (王文坚), Dun Mao (毛盾), Yong-Qiang Yu (于永强), Li Wang (王莉), Jun Xu (许俊), Ji-Gang Hu (胡继刚), and Lin-Bao Luo (罗林保)[a]
School of Electronic Science and Applied Physics and Anhui Provincial Key Laboratory of Advanced Functional Materials and Devices, Hefei University of Technology, Hefei, Anhui 230009, People's Republic of China

(Received 11 July 2013; accepted 17 October 2013; published online 4 November 2013)

We report on the rational synthesis of one-dimensional $Cu_{2-x}Se$ nanowires (NWs) *via* a solution method. Electrical analysis of $Cu_{2-x}Se$ NWs based memory device exhibits a stable and reproducible bipolar resistive switching behavior with a low set voltage (0.3–0.6 V), which can enable the device to write and erase data efficiently. Remarkably, the memory device has a record conductance switching ratio of 10^8, much higher than other devices ever reported. At last, a conducting filaments model is introduced to account for the resistive switching behavior. The totality of this study suggests that the $Cu_{2-x}Se$ NWs are promising building blocks for fabricating high-performance and low-consumption nonvolatile memory devices. © *2013 AIP Publishing LLC*. [http://dx.doi.org/10.1063/1.4828881]

Nowadays, tremendous efforts have been focused on the development of nanoscale electronic devices for possible non-Si technology replacement in future computer generations since the scaling limits to silicon transistors are almost exhausted.[1] To date, semiconductor nanostructures have found wide ranging devices applications including light emitting diodes (LEDs),[2] logic circuits,[3] memory devices,[4] photodetector,[5] solar cells,[6] and so on. Among these devices, memory devices, in particular resistive switching random access memory (ReRAM) devices employing stable resistance changes produced in response to the applied bias voltages, have attracted considerable attention due to their simple memory structures (metal/insulator/metal (MIM) structure, an electrochemical active metal, a solid electrolyte as an ion-conducting "I" layer, and a counter electrode made from an inert metal), low power consumption, high-speed operation, and nonvolatility. Furthermore, ion-migration-induced redox-type switching might offer huge potential for future high-density nonvolatile memories since it is the area in which nanoelectronics becomes intimately connected to nanoionics.[7]

Due to the high-mobility of Cu^+ ions, Cu_2S,[8,9] copper-doped carbon CuC (Ref. 10), and other copper-containing chalcogenide such as Cu-doped SiO_2 (Ref. 11) and Cu-doped MoO_3 (Ref. 12) have been extensively researched for copper-ionic based memory applications. The switching mechanism can be attributed to the creation and annihilation of localized conducting filaments under switching bias conditions. Copper selenide as one of the most important copper chalcogenides exists in a wide range of stoichiometric compositions (Cu_2Se, $CuSe_2$, Cu_3Se_2, Cu_5Se_4, and Cu_7Se_5) and nonstoichiometric compositions ($Cu_{2-x}Se$).[13] It has demonstrated potential applications in various fields such as solar cells,[14] optical filters,[15] thermoelectric and photoelectric transformers,[16] gas sensor,[17] and so on. In spite of these numerous progresses, there has been no report on $Cu_{2-x}Se$ nanowires (NWs) for memory devices application. Here, in this contribution, we report on the fabrication of nonvolatile memory devices made from $Cu_{2-x}Se$ NWs. Electrical analysis of the Cu/$Cu_{2-x}Se$/Au reveals obvious bipolar resistive switching behavior with very good reproducibility and a conductance ratio as high as 10^8. It is also found that the switching behavior is due to the creation and annihilation of the Cu filament within $Cu_{2-x}Se$ nanowires at different bias voltages.

The $Cu_{2-x}Se$ NWs employed in this work were synthesized using a modified solution method.[18] Briefly, a mixture of NaOH (1.29 g) and KOH (1.71 g) and 10 ml distilled water were put into a 50 ml flask and stirred until the formation of a homogeneous solution. Second, 1 mmol $CuCl_2{\cdot}2H_2O$, 0.5 mmol Se powder, and 2 ml of hydrazine hydrate were added into the flask. After ultrasonic agitation for about 30 min, the flask was sealed carefully and immersed into an oil bath. After reaction at 185 °C for 12 h, the flask was taken out and allowed to cool to room temperature. The black solid products were washed with hot deionized water and absolute ethanol several times and dried in a vacuum at 60 °C for 4 h. The morphologies and microstructures of the as-synthesized products were characterized by X-ray diffraction (XRD, Rigaku D/MAX2500V with Cu Kα radiation), scanning electron microscopy (SEM, JSM-6490LV), and high-resolution transmission electron microscopy (HRTEM, Philips CM 200 FEG). The composition of the $Cu_{2-x}Se$ nanowires was analyzed by energy-dispersive X-ray spectroscopy (EDS, Oxford INCA, attached to SEM).

To fabricate Cu/$Cu_{2-x}Se$/Au memory device, the as-synthesized $Cu_{2-x}Se$ NWs were dispersed uniformly onto SiO_2 (300 nm)-p^+-Si substrates with a desired density. Then photolithography, e-beam evaporation, and a lift-off process were employed to define an Au (50 nm) electrode on one end. Afterwards, an additional photolithography process was employed to define a Cu (50 nm) electrode on the other end of the nanowire. The device performance was evaluated by a semiconductor characterization system (Keithley 4200-SCS) at room temperature.

Fig. 1(a) depicts the XRD pattern of the as-synthesized products. All the diffraction peaks could be readily assigned

[a]Authors to whom correspondence should be addressed. Electronic addresses: cywu@hfut.edu.cn and luolb@hfut.edu.cn

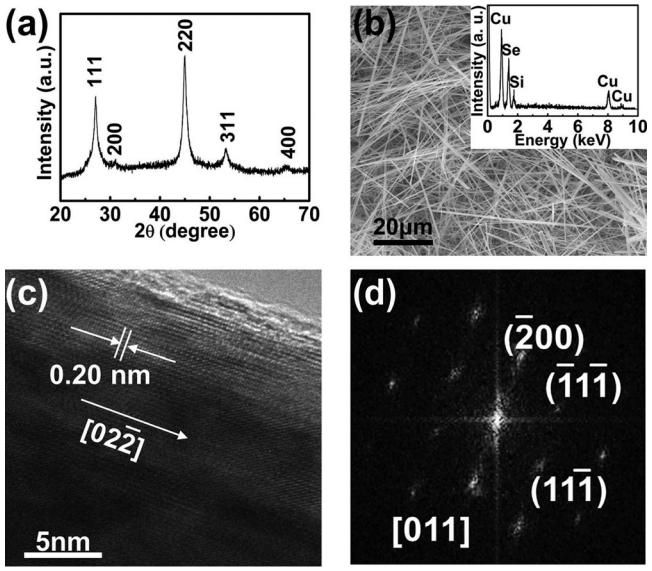

FIG. 1. Structure and morphology characterization of the $Cu_{2-x}Se$ nanowires. (a) XRD pattern, (b) SEM image, (c) HRTEM image, and (d) the corresponding FFT pattern. The inset in (b) shows the corresponding EDS pattern.

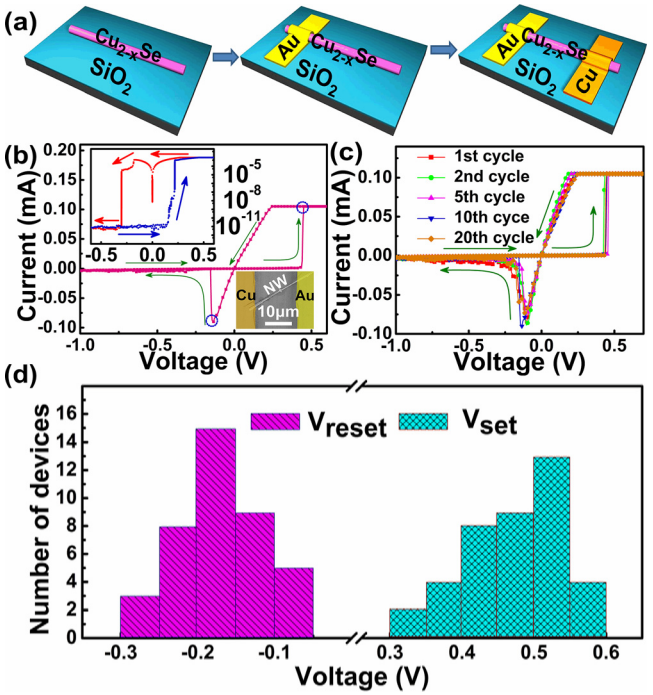

FIG. 2. (a) Schematic illustration of the step-wise process for fabrication of ReRAM nanodevice based on a single $Cu_{2-x}Se$ nanowire. (b) A typical *I–V* curve of as-fabricated nanodevice. The arrows indicate the voltage sweeping direction. The upper inset shows the *I–V* curve in a semilogarithmic plot, and the lower inset shows an SEM image of a typical nanodevice. (c) Representative *I–V* curves of a device measured for 20 times in sequence. (d) Histograms of the operation voltage distribution from 40 nanodevices (V_{set} and V_{reset} denote set and reset voltage, respectively).

to face-centered-cubic $Cu_{2-x}Se$ (JCPDS 06-0680). No evident impurity peaks from Cu and Cu_2O are observed, indicating that the products are of single phase and high purity. Notably, the peak intensity of the (220) is much stronger than that in the standard JCPDS card, which may imply the possible preferential orientation growth. The SEM image in Fig. 1(b) shows that the product consists of a large quantity of ultra-long nanostructures, with diameters in the range of 300–800 nm and lengths of more than 40 μm. Further EDS spectrum (inset in Fig. 1(b)) reveals an atomic ratio of Cu:Se ~1.78:1, in consistency with the nonstoichiometric composition of the products ($Cu_{2-x}Se$). Note that the Si peak in the EDS spectrum stems from the Si substrate. Further HRTEM image (Fig. 1(c)) and the corresponding fast Fourier transform (FFT) pattern (Fig. 1(d)) recorded at a typical nanowire reveal that the as-synthesized $Cu_{2-x}Se$ nanowire is single crystalline with face-centered cubic structure. In addition, the *d-spacing* (0.20 nm) between adjacent lattice planes corresponds to the [02$\bar{2}$] growth direction, which agrees well with the unusual strong reflection peak observed in XRD patterns.

The scheme in Fig. 2(a) illustrates the step-wise process to fabricate the Cu/$Cu_{2-x}Se$/Au nanodevices. The distance between the two parallel electrodes is ~15 μm (cf., the inset in Fig. 2(b)). Fig. 2(b) shows the typical current (*I*)-voltage (*V*) characteristic of the as-fabricated nanodevice measured by a dc voltage sweeping with a sweeping loop −1 V → 0 V → 1 V → 0 V → −1 V (the bias was applied to the Cu electrode and the Au electrode was grounded). Apparently, the device shows a typical bipolar resistive switching behavior. That is, when the voltage swept from −1 V to 1 V, the device would be switched suddenly from the off state (high resistance) to the on state (low resistance) at the set voltage (V_{set}) 0.44 V, with a response speed less than 0.1 s. It would retain the on state until a reverse voltage was applied to switch it back to the off state. Specifically, the off state occurred at the reset voltage (V_{reset}) −0.14 V when the voltage swept back from 1 V to −1 V. According to the *I–V* curve in a semilogarithmic plot shown in the upper inset in Fig. 2(b), the conductance ratio of the on/off states is up to 10^8 at 0.1 V, which is much higher than that of previously reported Cu^+-based resistive switching devices such as Cu_2S films (10^6),[8] Cu_2S and Cu-Pc bilayer films (10^3–10^4).[9] As a matter of fact, this conductance ratio can be further improved considering that the current compliance was fixed at 1 mA to avoid the device failure by high current. Moreover, though the set voltage of the present device is comparable to the device mentioned above, yet it is remarkably lower than that of memories devices based on other nanostructures such as ZnS nanoribbon,[19] Si/α-Si core/shell nanowires,[20] and ZnO nanowires.[21] In addition to the higher conductance ratio and low reset voltage, the present device exhibits excellent reproducibility as well. Fig. 2(c) shows the *I-V* curves for 20 sequential cycles, the high coincidence of the initial cycle, and the twenty subsequent cycles which confirmed that the resistive switching between the on and off state is reproducible. Notably, no apparent difference between the first set voltage ($V_{set,form}$) and the following set voltage (V_{set}) has been observed during our experiment. We attribute this subtle difference to the high mobility of Cu^+. Furthermore, the statistical histograms of the operation voltages (V_{set} and V_{reset}) of over than 40 devices in Fig. 2(d) reveal that all devices exhibited similar bipolar resistive switching behavior, with the mean values 0.48 V and −0.16 V, for V_{set} and V_{reset}, respectively. The relatively narrow V_{set} distribution at 0.3–0.6 V and V_{reset} at −0.3 ~ −0.05 V suggest high uniformity and excellent reproducibility of the devices.

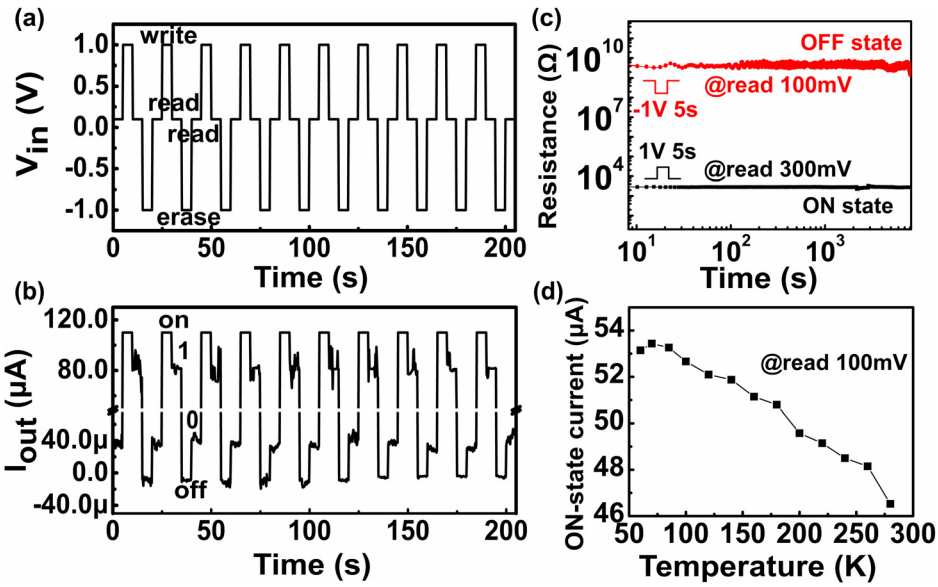

FIG. 3. Switching property of the device tested by cycling of write-read-erase-read operation. (a) The input voltage (V_{in}), (b) the response current (I_{out}). (c) The retention property of R_{high} and R_{low}, which demonstrates no degradation for up to 8000 s. (d) The change of the on-state current at various low temperatures.

To evaluate the capability of the present device for memory device application, a coherent write-read-erase-read process was carried out under a programmed pulsed cycle voltage at a pulse step of 5 s. Figs. 3(a) and 3(b) display the reversible switching at room temperature with ten read/write circles. Obviously, one can see that on state can be obtained when 1 V was applied. To read the on state, a small voltage of 0.1 V was introduced to the device after the turn-on process, and the response current in the device was measured to be ~0.08 mA. The resistance of the device is about 1.7×10^3 Ω. Such a low resistance state (LRS) corresponds to write data into the device. On the contrary, one needs to apply −1 V voltage in order to switch off the device with response current of 20–50 pA with some noise. This high resistance state (HRS) followed by a 0.1 V to probe the state can serve to erase data from the device. Note that the labels "1" and "0" in Fig. 3(b) were designated as the low and high resistance states, respectively. The write-read-erase-read cycles can be repeated for more than 100 times, suggesting great potential as a nonvolatile memory device. The stable conductance ratio of the on/off states can be ascribed to the sufficiently long pulse width (5 s) for the creation and annihilation of the conducting paths inside the $Cu_{2-x}Se$ nanowire.[9] Furthermore, the retention characteristics of the on state and the off state at room temperature in Fig. 3(c) indicate that neither the on state nor the off state shows apparent degradation for at least 8×10^3 s, indicative of the excellent nonvolatility of the device. It appears that the on state is much more stable than the off state since it was controlled by the current compliance. Detailed comparison of the key memory parameters of our devices with previously reported memories was shown in Table I.

Previously, a conducting filament model was proposed to account for the bipolar switching behavior of copper-ionic materials based memory devices.[8–12] In fact, this model could apply to our $Cu_{2-x}Se$ nanostructure based memory as well. As illustrated in Fig. 4, there is no conducting filament in the $Cu_{2-x}Se$ nanowire at zero applying voltages. The conductance is low, and the device is on the off state. When applying a positive voltage larger than the set voltage (1 V in our experiments) on the Cu electrode, the high-mobility Cu^+ cations within the $Cu_{2-x}Se$ nanowire will migrate towards the cathode made of inert Au, where they are reduced by electrons. The Cu atoms will keep growing till the metal filament reaches the anode, whereby the device was switched to on state. It should be pointed out that the Cu filament thus formed is highly electrochemically active, and they can be oxidized and dissolved into the $Cu_{2-x}Se$ nanowire. In other words, the creation and annihilation of the Cu is a reversible process which can be described as follows:

$$Cu^+(Cu_{2-x}Se) + e^- \underset{\text{Oxidation}}{\overset{\text{Reduction}}{\rightleftharpoons}} Cu.$$

TABLE I. Comparison of the key memory parameters for the memories from the previous reports and the present work.

Memory media	Operation mechanism	V_{set}	I_{on}/I_{off}	Retention time
$Cu_{2-x}Se$ NW	Conductance filament	0.3–0.6 V	$>10^8$	$>8 \times 10^3$ s
Cu_2S film[a]	Conductance filament	<0.3 V	$>10^6$	…
p-ZnS/n-Si heterojunction[b]	ZnS/-Si interface	2.7–3.3 V	$>10^6$	$>10^5$ s
Si/a-Si × Ag NW[c]	Conductance filament	~3 V	$>10^4$	>2 weeks
ZnO NW coated with ferroelectric NPs[d]	Ferroelectric FET	~15 V	$>10^4$	$>4 \times 10^4$ s

[a]See Ref. 8.
[b]See Ref. 19.
[c]See Ref. 20.
[d]See Ref. 21.

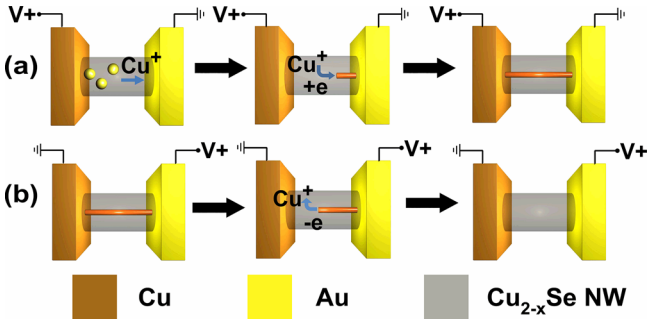

FIG. 4. Schematic drawings of the operating mechanism: (a) creation and (b) annihilation of the conducting filaments, respectively.

On changing the polarity of the bias voltage (as shown in Fig. 4(b)), Cu atoms dissolve at the edge of the metal filament, eventually annihilating the filament so that the device is switched back to its off state. Considering that the chemical reaction ideally does not cause any damage to the MIM system, the switch may in principle be expected to work indefinitely.[7]

The conducting filament model was experimentally verified by the variation of the on-state resistance at temperature in Fig. 3(d). The increase of current with decreasing temperature suggests that the conducting filament is composed of metallic materials, as opposed to semiconductor. Assuming the conducting metallic filament formed in the $Cu_{2-x}Se$ nanowire to be pure copper and treating the resistance as a single filament for simplification, the equivalent diameter of the copper filament can be estimated to be $\sim$14 nm, comparable to the reported values.[9] This consistence further proves that the conducting filament mechanism plays an important role in forming resistive switching behavior.

In summary, $Cu_{2-x}Se$ NWs with diameters in the range of 300–800 nm and lengths of more than 40 μm were synthesized through a solution reaction approach. Electrical analysis reveals that the Cu/$Cu_{2-x}Se$/Au memory device exhibits typical bipolar resistive switching behavior with low set voltage in the range from 0.3 to 0.6 V, a large conductance switching ratio as high as 10^8, and a retention time of more than 8×10^3 s. Such a remarkable memory characteristics can be attributed to the creation and annihilation of the Cu filament within $Cu_{2-x}Se$ nanowires at different bias voltages. This study proves that $Cu_{2-x}Se$ nanostructures have great potential for future high performance nonvolatile memories application.

This work was supported by the National Natural Science Foundation of China (NSFC, Nos. 20901021, 51172151, 61106010, 21301044, and 21101051), the Natural Science Foundation of Anhui Province of China (No. 11040606Q26), and the Fundamental Research Funds for the Central Universities (Nos. 2013HGXJ0195 and 2013HGCH0012).

[1]S. E. Thompson and S. Parthasarathy, Mater. Today **9**, 20 (2006).
[2]J. J. Cai, J. S. Jie, P. Jiang, D. Wu, C. Xie, C. Y. Wu, Z. Wang, Y. Q. Yu, L. Wang, X. W. Zhang, Q. Peng, and Y. Jiang, Phys. Chem. Chem. Phys. **13**, 14663 (2011).
[3]C. Collier, E. Wong, M. Belohradský, F. Raymo, J. Stoddart, P. Kuekes, R. Williams, and J. Heath, Science **285**, 391 (1999).
[4]C. Xie, B. Nie, L. Zhu, L. H. Zeng, Y. Q. Yu, X. H. Wang, Q. L. Fang, L. B. Luo, and Y. C. Wu, Nanotechnol. **24**, 355203 (2013).
[5]Y. Q. Yu, J. S. Jie, P. Jiang, L. Wang, C. Y. Wu, Q. Peng, X. W. Zhang, Z. Wang, C. Xie, D. Wu, and Y. Jiang, J. Mater. Chem. **21**, 12632 (2011).
[6]J. Y. Tang, Z. Y. Huo, S. Brittman, H. W. Gao, and P. D. Yang, Nat. Nanotechnol. **6**, 568 (2011).
[7]R. Waser and M. Aono, Nat. Mater. **6**, 833 (2007).
[8]T. Sakamoto, H. Sunamura, H. Kawaura, T. Hasegawa, T. Nakayama, and M. Aono, Appl. Phys. Lett. **82**, 3032 (2003).
[9]L. Chen, Y. D. Xia, X. F. Liang, K. B. Yin, J. Yin, Z. G. Liu, and Y. Chen, Appl. Phys. Lett. **91**, 073511 (2007).
[10]M. Pyun, H. Choi, J.-B. Park, D. Lee, M. Hasan, R. Dong, S.-J. Jung, J. Lee, D.-J. Seong, and J. Yoon, Appl. Phys. Lett. **93**, 212907 (2008).
[11]C. Schindler, S. C. P. Thermadam, R. Waser, and M. N. Kozicki, IEEE Trans. Electron Devices **54**, 2762 (2007).
[12]D. Lee, D.-J. Seong, H. J. Choi, I. Jo, F. Xiang, R. Dong, S. Oh, S. Seo, and H. Hwang, Appl. Phys. Lett. **90**, 122104 (2007).
[13]P. Kumar, K. Singh, and O. N. Srivastava, J. Cryst. Growth **312**, 2804 (2010).
[14]A. Hermann and L. Fabick, J. Cryst. Grow. **61**, 658 (1983).
[15]A. A. Korzhuev, Fiz. Khim Obrab. Mater. **3**, 131 (1991).
[16]V. Bhuse, P. Hankare, K. Garadkar, and A. Khomane, Mater. Chem. Phys. **80**, 82 (2003).
[17]J. Xu, W. X. Zhang, Z. H. Yang, S. X. Ding, C. Y. Zeng, L. L. Chen, Q. Wang, and S. H. Yang, Adv. Funct. Mater. **19**, 1759 (2009).
[18]Y. Zhang, C. G. Hu, C. H. Zheng, Y. Xi, and B. Y. Wan, J. Phys. Chem. C **114**, 14849 (2010).
[19]Y. Q. Yu, Y. Jiang, P. Jiang, Y. G. Zhang, D. Wu, Z. F. Zhu, Q. Liang, S. R. Chen, Y. Zhang, and J. S. Jie, J. Mater. Chem. C **1**, 1238 (2013).
[20]Y. J. Dong, G. H. Yu, M. C. McAlpine, W. Lu, and C. M. Lieber, Nano Lett. **8**, 386 (2008).
[21]J. I. Sohn, S. S. Choi, S. M. Morris, J. S. Bendall, H. J. Coles, W.-K. Hong, G. Jo, T. Lee, and M. E. Welland, Nano Lett. **10**, 4316 (2010).